MOLECULAR AND CELLULAR BIOLOGY, Jan. 2005, p. 414–421 Vol. 25, No. 1
0270-7306/05/$08.00+0 doi:10.1128/MCB.25.1.414–421.2005

WISP3, the Gene Responsible for the Human Skeletal Disease Progressive Pseudorheumatoid Dysplasia, Is Not Essential for Skeletal Function in Mice

Wendy E. Kutz,[1] Yaoqin Gong,[1]† and Matthew L. Warman[1,2,3]*

Departments of Genetics[1] and Pediatrics,[2] Case Western Reserve University, and Center for Human Genetics,[3] University Hospitals of Cleveland, Cleveland, Ohio

Received 28 May 2004/Returned for modification 14 July 2004/Accepted 23 September 2004

In humans, loss-of-function mutations in *WISP3* cause the autosomal recessive skeletal disease progressive pseudorheumatoid dysplasia (PPD) (Online Mendelian Inheritance in Man database number 208230). *WISP3* encodes Wnt1-inducible signaling protein 3, a cysteine-rich, multidomain, secreted protein, whose paralogous CCN (connective tissue growth factor/cysteine-rich protein 61/nephroblastoma overexpressed) family members have been implicated in diverse biologic processes including skeletal, vascular, and neural development. To understand the role of *WISP3* in the skeleton, we targeted the *Wisp3* gene in mice by creating a mutant allele comparable to that which causes human disease. We also created transgenic mice that overexpress human WISP3 in cartilage. Surprisingly, homozygous *Wisp3* mutant mice appear normal and do not recapitulate any of the morphological, radiographic, or histological abnormalities seen in patients with PPD. Mice that overexpress WISP3 are also normal. We conclude, that in contrast to humans, *Wisp3* is not an essential participant during skeletal growth or homeostasis in mice.

The CCN (connective tissue growth factor/cysteine-rich protein 61/nephroblastoma overexpressed) protein family comprises six cysteine-rich, multidomain-containing, secreted proteins (1, 19, 20). To date, only one CCN family member, Wnt1-inducible signaling protein 3 (WISP3/CCN6) has been associated with a human genetic disease. Mutations in *WISP3* cause progressive pseudorheumatoid dysplasia (PPD) (4, 8), an autosomal recessive form of a spondyloepiphyseal dysplasia tarda. Individuals with PPD appear normal at birth, have subtle clinical symptoms by 3 years of age, manifest radiologic changes of the axial and appendicular skeleton by 5 years of age, and develop severe degenerative joint disease necessitating joint replacement surgery by their second decade of life (5, 21, 24, 27). Radiologically, in addition to platyspondyly, young patients with PPD have multiple sites of epiphyseal enlargement compared to age- and gender-matched controls (12, 17). Histological examination shows that articular cartilage retrieved at the time of joint replacement surgery from patients with PPD is indistinguishable from that seen in common end-stage osteoarthritis (W. Kutz et al., unpublished data). Individuals with PPD have no organ involvement outside of their skeletal system. Consequently, in humans, the principal role of WISP3 appears to involve skeletal growth and cartilage homeostasis.

We disrupted the *Wisp3* gene in mice to create an animal model of Wisp3 deficiency and thus delineate the precise role of this protein in the skeleton. We found that homozygous *Wisp3* mutant (*Wisp3*$^{-/-}$) mice do not recapitulate any of the features that have been observed in patients with PPD. We also created transgenic mice that overexpress human WISP3 in cartilage; these mice are also normal. Our results suggest that although *WISP3* is critical for normal skeletal function in humans, *Wisp3* is not essential in mice.

MATERIALS AND METHODS

Construction of the *Wisp3* targeting vector and generation of *Wisp3* mutant mice. A mouse genomic DNA library was screened at low stringency with human *WISP3* cDNA. A 17-kb phage clone containing exons 2 to 5 and adjoining upstream and downstream sequences was isolated. The exonic sequences in this phage clone were used to design primers that could amplify a correctly spliced cDNA by reverse transcriptase PCR (RT-PCR) using embryonic stem (ES) cell total RNA as a template. This phage DNA was then used as a template to PCR amplify the 5′ and 3′ targeting arms for a vector that also contains the coding sequence for β-galactosidase (*lacZ*) and neomycin resistance. The targeting scheme is depicted below (see Fig. 2A). We also amplified the noncoding sequence within the *Wisp3* locus to identify polymorphisms between the C57BL/6J and *Mus spretus* mouse strains. One polymorphism was used to map murine *Wisp3* to a region on chromosome 10 that is orthologous to the human map location of *WISP3* on chromosome 6 (data not shown).

Homologous recombination in mouse 129/SvEv ES cells was performed by standard methods. Correct targeting was confirmed using a 650-bp probe from outside of the 3′ targeting arm, which recognizes an 11-kb wild-type EcoRI fragment and a 6-kb mutant allele EcoRI fragment. Correct targeting at the 5′ end was confirmed by sequencing a PCR product obtained with a primer upstream of the targeting arm and one within the targeting vector's *lacZ* gene. Positive clones were microinjected into C57BL/6J blastocysts and implanted into CD-1 pseudopregnant females. Six-week-old male chimeras were mated with NIH Black Swiss females to check for germ line transmission. Males with germ line transmission were bred with 129/SvEv females to establish an inbred strain of *Wisp3* mutant mice. Institutional Animal Care and Use Committee standards and procedures for mouse research were followed.

RT-PCR analyses to detect the presence of wild-type and *Wisp3-lacZ* fusion transcripts. Kidneys from wild-type (*Wisp3*$^{+/+}$), heterozygous mutant (*Wisp3*$^{+/-}$), and homozygous mutant (*Wisp3*$^{-/-}$) mice were isolated and total RNA extracted with Trizol (Invitrogen). cDNA was synthesized with 4 μg of total RNA and oligo(dT) with the SuperScript First Strand Synthesis system for RT-PCR (Invitrogen). A total of 2 μl of cDNA was used to PCR amplify wild-type and *Wisp3-lacZ* fusion transcripts. Amplification of wild-type (311 bp) and mutant (308 bp) *Wisp3* transcripts utilized a common forward primer,

* Corresponding author. Mailing address: Department of Genetics, Case Western Reserve University, 2109 Adelbert Rd., BRB 719, Cleveland, OH 44106-4955. Phone: (216) 368-4919. Fax: (216) 368-5857. E-mail: mlw14@po.cwru.edu.

† Present address: Shandong Medical University, Jinan, China.

WmRNA3F (5′-GCAGCATTGGAGGTGTATCA), and allele-specific reverse primers, WmWTrnaR (5′-TCACACAGAGGCAGCTGAAC) and lacZ-1R (5′-CCATGCTCCCCACTTTGCGT). PCR conditions included initial denaturation at 95°C for 3 min; 40 cycles of denaturation (95°C for 30 s), annealing (60°C for 45 s), and elongation (72°C for 50 s); and 10 min of elongation at 72°C.

Testing the *Wisp3-lacZ* fusion product for β-galactosidase activity. The 5′ end of the *Wisp3-lacZ* fusion mRNA was amplified by RT-PCR from *Wisp3*$^{+/-}$ kidney total RNA. The product contained correctly spliced *Wisp3* exons 1 and 2 and part of exon 3 attached in frame with *lacZ*. This fragment was then subcloned with the SalI site present in *lacZ* and in the *Wisp3-lacZ* fusion to recreate the product of the targeted allele in the mammalian expression vector pcDNA3. We transfected 1 μg of this vector into 75% confluent COS-7 cells plated on four-well chamber slides with FuGENE 6 (Roche Diagnostics Corp.) according to the manufacturer's instructions. β-Galactosidase expression was detected by in situ staining with X-Gal (5-bromo-4-chloro-3-indolyl-β-galactoside) substrate. Cells were rinsed with Dulbecco's phosphate-buffered saline (DPBS; Mediatech, Inc.) 24 h after transfection and fixed with 2% formaldehyde and 0.2% glutaraldehyde in DPBS. Following fixation, cells were rinsed twice with DPBS before being stained with 0.1% X-Gal in DPBS containing 5 mM potassium ferricyanide and 2 mM $MgCl_2$. Cells were visualized with a Leica DMLB microscope (Leica Microsystems, Inc.), and images were captured with a Spot camera and software (Diagnostics Instruments, Inc.).

Radiologic and histological analyses of wild-type, mutant, and transgenic mice. Immediately following sacrifice by CO_2, animals were x-rayed at 30 mPv for 1.5 min with a Faxitron on Kodak X-Omat AR scientific imaging film (Eastman Kodak Company). Images were captured with an Optronics LX-450 camera attached to a Leica MZFLIII microscope (Leica Microsystems, Inc.) with Scion Image 1.62a software (Scion Corp.).

For histology, knee joints were fixed in 10% buffered formalin (Fisher Scientific) before being placed in Tissue-Tek biopsy cassettes (Sakura Finetek U.S.A., Inc.) and being decalcified with 10% EDTA (pH 7.1) for 1 week. Samples were then processed and embedded in paraffin. Serial sagittal or coronal sections (7 μm) traversing the entire joint were collected on Fisherbrand Superfrost/Plus slides (Fisher Scientific) and used for histochemical staining. Images were viewed on a Leica DMLB microscope (Leica Microsystems, Inc.) and captured with a Spot Camera and software (Diagnostics Instruments, Inc.). For analysis of knee osteoarthritis, every fifth slide collected (~140 μm apart) was stained with toluidine blue and photographed. Two individuals viewed the slides and pictures separately. Mice showing signs of cartilage surface fibrillation, loss of proteoglycan staining, synovial hyperplasia, and "chondrification" of posterior connective tissues were scored as having severe osteoarthritis.

Skeletal preparations of wild-type and mutant mice. Seven-day-old mice were euthanized in a CO_2 chamber and placed in a hot-water bath for 2 to 3 min to facilitate skin removal. Deskinned pups were eviscerated and fixed in 95% ethanol (EtOH) overnight (O/N) at 4°C. Specimens were then stained with 30 mg of Alcian blue in 80 ml of 95% EtOH and 20 ml of glacial acetic acid O/N at room temperature. Skeletons were then washed twice with 95% EtOH and left in 95% EtOH O/N at 4°C before being stained with alizarin red (5 mg in 100 ml of 1% KOH) O/N at room temperature. Clearing was done by placing pups in 0.5% KOH for 8 to 12 h at room temperature, 0.5% KOH–glycerol (67:33) O/N, and 0.5% KOH–glycerol (50:50) for several days until the pups sank. Skeletal preparations were then moved into 0.5% KOH–glycerol (33:67) solution before storage in 100% glycerol. Photographs were taken as described for the x-rays. Stained front and hind paws, as well as knee joints, were assessed for their degree of ossification. Animals were examined for the presence or absence of ossified carpal and tarsal bones, and if present the number of bones was recorded. The knees were scored for secondary centers of ossification in the femoral condyle and tibial plateau. The number of carpal, tarsal, and knee ossification sites were then compared between wild-type and *Wisp3*$^{-/-}$ mice.

Voluntary running wheel experiments. Eight-week-old wild-type and *Wisp3*$^{-/-}$ male mice were individually housed in rat and/or guinea pig cages (Allentown Caging Equipment Co.) that contained a S.A.M. jogging wheel (diameter, 4.5 in.) (Penn-Plex, Inc.) with a spoke magnet (Sigma Sport) attached. Each animal had unrestricted access to the jogging wheel, food, and water for 8 or 12 months. Daily running times (in hours) and distances (in kilometers) were recorded with Sigma Sport BC800 bike computers and reset daily.

***WISP3* transgenic (*WISP3*^{TG}) mouse construct.** Full-length human *WISP3* cDNA was cloned into pKN185 (a gift from Yoshihiko Yamada) with NotI sites, placing it under the control of the collagen type II (*Col2a1*) promoter and enhancer. Transgenic insert (2 ng/μl) was injected into C57BL/6J pronuclei. Swollen, nonlysed pronuclei were transferred to oviducts of pseudopregnant CD-1 females (Case Transgenic and Targeting Facility, Cleveland, Ohio). *WISP3*^{TG} animals were identified by Southern blot analysis with a ^{32}P-random-prime-labeled (Amersham Pharmacia Biotech) full-length *WISP3* cDNA probe and genomic tail DNA (3 μg) digested with PstI to detect a 1-kb fragment. Males positive for the 1-kb *WISP3*^{TG} fragment were mated with 129/SvEv wild-type females to test for transgene propagation to offspring.

Determination of WISP3^{TG} expression. Knee-joint cartilage, costal cartilage, kidney, and testes were isolated from 3-week-old wild-type and *WISP3*^{TG} mice. Total RNA extraction with TRIzol (Invitrogen) was performed following the manufacturer's instructions. RNA (10 μg/lane) was loaded onto a formaldehyde-agarose gel and electrophoresed as previously detailed (22). Full-length *WISP3* cDNA was ^{32}P-random-prime-labeled with the Megaprime DNA labeling system (Amersham Pharmacia Biotech) and hybridized to the RNA filter to detect 1.2-kb *WISP3* transcripts. Ethidium bromide staining of the 18S rRNA subunit was used to confirm equivalency of RNA loading.

WISP3 carboxy-terminal antibody production and purification. The WISP3 C-terminal domain polypeptide sequence, VCQRDCREPGDIFSE, was selected for polyclonal antibody production and synthesized (Princeton Biomolecules, Langhorne, Pa.) in keyhole limpet hemocyanin-conjugated and unconjugated forms. The peptides were shipped to Covance (Denver, Pa.), and keyhole limpet hemocyanin-conjugated WISP3 peptide was injected into two New Zealand White rabbits for antibody production following Covance's standard procedures. Pretest, test, and production bleeds were tested by enzyme-linked immunosorbent assay (Covance) for recognition of unconjugated WISP3 peptide and shipped to us for Western blot analysis of antibody against recombinant WISP3 protein. C-terminal WISP3 antibody (W3-C) capable of detecting recombinant WISP3 protein was then purified with an antigen peptide column. Unconjugated WISP3 peptide (0.5 mg/500 μl of DPBS) was bound to 2 ml of *N*-hydroxysuccinimide-activated Sepharose beads (Amersham Biosciences) following the recommended instructions and then packed in a 10-ml Poly-Prep chromatography column (Bio-Rad Laboratories). Four milliliters of production bleed serum was then diluted with 4 ml of DPBS before being added to the antigen column O/N at 4°C with constant rotation. The following day, the column was drained by gravity and washed three times with DPBS (8 ml/wash). Antibody was then eluted off the column with 0.1 M glycine (pH 2.7) and neutralized with 1 M Tris (pH 10). Twelve 1-ml fractions were collected from each round of purification and tested against recombinant WISP3 protein by Western blot analysis.

Analysis of WISP3 protein expression in *WISP3*^{TG} mice. Protein was extracted from pulverized femoral head cartilage of wild-type and *WISP3*^{TG} mice with 8 M urea O/N at 4°C. Protein extract was mixed with an equal volume of 2× sodium dodecyl sulfate (SDS) sample loading buffer, boiled for 5 min in the presence of 5% β-mercaptoethanol, and separated by SDS-polyacrylamide gel electrophoresis with the Mini Protean 3 system (Bio-Rad Laboratories). Separated proteins were transferred to an Immobilon P membrane (Millipore Corp.). Following transfer, membranes were blocked in 4% nonfat dry milk–Tris-buffered saline. WISP3 protein was detected with the rabbit polyclonal WISP3 primary antibody W3-C (1:500 dilution) with goat anti-rabbit horseradish peroxidase-conjugated immunoglobulin G (heavy plus light chains) (Pierce) as the secondary antibody. Development of blots with the ECL plus Western Blotting Detection System (Amersham Biosciences) was followed by exposure to X-Omat AR film (Eastman Kodak Company) for the detection of protein signal.

Immunohistochemistry of *WISP3*^{TG} cartilage. Two-day old wild-type, *Wisp3*$^{-/-}$, and *WISP3*^{TG} pups were sacrificed with CO_2 and fixed with 4% paraformaldehyde (Sigma) for 4 h at 4°C. Front and hind limbs were then isolated, rinsed in ice-cold DPBS, and put through a gradient of 10, 15, and 30% sucrose–DPBS until the limbs sank. Samples were then embedded in Tissue Tek OCT compound (Sakura Finetek U.S.A., Inc.), sectioned on a Leica CM 3050 cryostat (Leica Microsystems, Inc.) in12-μm increments, and collected on Fisherbrand Superfrost/Plus microscope slides (Fisher Scientific) for storage at −80°C. Before being immunostained, slides were dried for 15 min at room temperature, fixed in 4% paraformaldehyde for 10 min, and digested with bovine IV-S hyaluronidase (Sigma) (2 mg/ml in DPBS; pH 5) for 30 min. Three 5-min washes of DPBS followed both the fixation and digestion steps. Slides were then pretreated with blocking serum (1.5% normal goat serum [Vector Laboratories]–DPBS) for 30 min. Rabbit polyclonal W3-C primary antibody (1:100 dilution) was added to the blocking serum and incubated with the sections O/N at 4°C. Additional slides were incubated with preimmune serum or secondary antibody alone to serve as controls. Slides were washed three times with DPBS (5 min each) before applying Alexa Fluor 594 goat anti-rabbit immunoglobulin G (heavy plus light chains) (Molecular Probes) in blocking serum (1:200 dilution). Three additional washes of DPBS followed before slides were mounted with Vectashield mounting medium containing DAPI (4′,6-diamidino-2-phenylindole) (Vector Laboratories). Images were visualized on a Leica DMLB microscope and captured with a Spot camera and software (Diagnostics Instruments, Inc.).

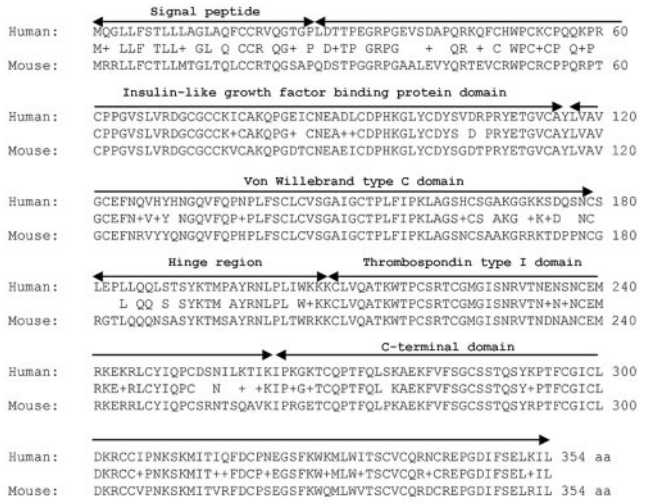

FIG. 1. Comparison of human WISP3 and mouse Wisp3 protein sequences with single-letter amino acid codes. The human and mouse proteins are 87% similar and 78% identical at the amino acid level, based upon BLASTp alignment with a BLOSUM62 matrix. The middle sequence indicates the identical and similar (+) amino acid residues. Peptide domains are labeled with black arrows.

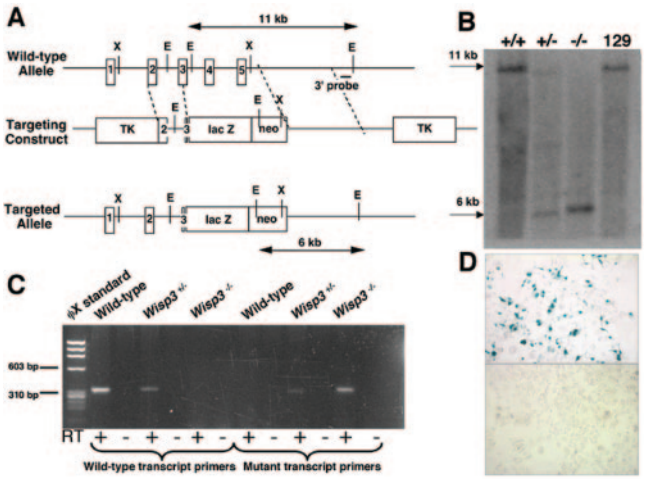

FIG. 2. Targeted disruption of *Wisp3* in mice. (A) Structure of the wild-type allele, the targeting construct, and the targeted allele (*Wisp3-lacZ*). EcoRI restriction enzyme sites (E) and restriction fragment lengths are noted. Black outlined boxes indicate individual exons. (B) Southern blot analysis of EcoRI-digested genomic DNA from control 129/SvEv mice and from $Wisp3^{+/+}$, $Wisp3^{+/-}$, and $Wisp3^{-/-}$ offspring of $Wisp3^{+/-}$ parents. Wild-type *Wisp3* alleles are 11 kb and mutant alleles are 6 kb. (C) RT-PCR amplimers of wild-type and *Wisp3-lacZ* (mutant) transcripts from $Wisp3^{+/+}$ (wild-type), $Wisp3^{+/-}$, and $Wisp3^{-/-}$ mice. Wild-type transcript primers yielded the expected 311-bp product from wild-type and $Wisp3^{+/-}$ cartilage, but not from $Wisp3^{-/-}$ $Wisp3^{-/-}$ cartilage. Conversely, amplification with *Wisp3-lacZ* mutant transcript primers yielded the expected 308-bp product from $Wisp3^{+/-}$ and $Wisp3^{-/-}$ cartilage but not from wild-type cartilage. No amplimers were observed when non-reverse-transcribed RNA (RT −) was used as PCR template. (D) Photomicrographs (magnification, ×400) of Cos-7 cells transiently transfected with a vector expressing the Wisp3-lacZ fusion protein exhibit β-galactosidase activity (top), while nontransfected cells do not (bottom).

RESULTS

Mouse *Wisp3* mRNA is orthologous to human *WISP3*. The mouse *Wisp3* coding sequence is 82% identical to human *WISP3* at the nucleotide level and 87% similar (78% identical) at the amino acid level (Fig. 1). Sequence similarity is least conserved within the signal peptide and hinge region and most conserved within the protein's four putative functional domains (Fig. 1). Amino acid similarity (and identity) between mouse and human is 82% (72%), 91% (83%), 90% (81%), and 98% (87%) for the IGFBP, vWC, TSP1, and CT domains, respectively. Genomic sequence for mouse *Wisp3* is contained on chromosome 10 between the genes *Fyn* and *Tube* (http://genome.ucsc.edu). This synteny is identical to that of human *WISP3* on chromosome 6q.

Mouse *Wisp3* mRNA is not detected by Northern blotting or by in situ hybridization. Although it is possible to amplify correctly spliced *Wisp3* mRNA by RT-PCR from male and female mouse tissues including cartilage, kidney, and testis obtained at 7 days, 1 month, and 1 year of age, we could not detect *Wisp3* mRNA on mouse embryonic or multitissue Northern blots (data not shown). Similarly, we could not detect human *WISP3* mRNA on a commercially available multitissue Northern blot or on Northern blots containing poly(A)$^+$ RNA from several cell lines, including a human chondrosarcoma cell line (HCSC), a human mammary epithelial cell line (HME) (a gift from Celina Kleer), and the human osteoblastic cell lines U-2 OS, MG-63, and Saos-2 (American Type Culture Collection). We have also been unable to detect *Wisp3* mRNA in developing limb structures of female and male mice, including bone, growth plate, and cartilage, by in situ hybridization at embryonic days 12, 14, 16, and 18 and postnatal days 1, 2, and 7.

Targeting of the *Wisp3* locus in mice. Multiple human disease-causing truncation mutations, including one that removes the protein's terminal 14 amino acids, indicate that full-length WISP3 is required for proper biological function (reference 8; Kutz et al., unpublished). We created a *Wisp3* mutant allele that is comparable to human disease-causing mutations by truncating the protein after the IGFBP domain. The mutation removes the vWF, TSP, and C-terminal domains of *Wisp3*. Because Wisp3 expression is not detectable by standard methods, we engineered the mutant *Wisp3* allele to produce a fusion protein that has β-galactosidase activity under the control of the endogenous upstream *Wisp3* regulatory sequence (Fig. 2A). We confirmed correct targeting of *Wisp3* in 129/SvEv ES cells and in wild-type ($Wisp3^{+/+}$), heterozygous ($Wisp3^{+/-}$), and homozygous mutant ($Wisp3^{-/-}$) liveborn mice by Southern blotting (Fig. 2B). We found that the mutant *Wisp3* allele produces a spliced mRNA that contains the *lacZ* fusion by RT-PCR (Fig. 2C), and we showed that the Wisp3-lacZ fusion protein retains β-galactosidase activity by transiently transfection of 293-EBNA cells with a cDNA expression vector encoding the fusion protein (Fig. 2D).

Litters born to $Wisp3^{+/-}$ mice were of normal size and had pups with Mendelian ratios of $Wisp3^{+/+}$, $Wisp3^{+/-}$, and $Wisp3^{-/-}$. $Wisp3^{-/-}$ mice did not differ in size or weight from their littermates at birth or at the time of sacrifice. Sexually mature female and male $Wisp3^{-/-}$ mice were fertile and capable of producing litters of normal size and numbers. Life spans seemed unchanged in $Wisp3^{-/-}$ animals when compared

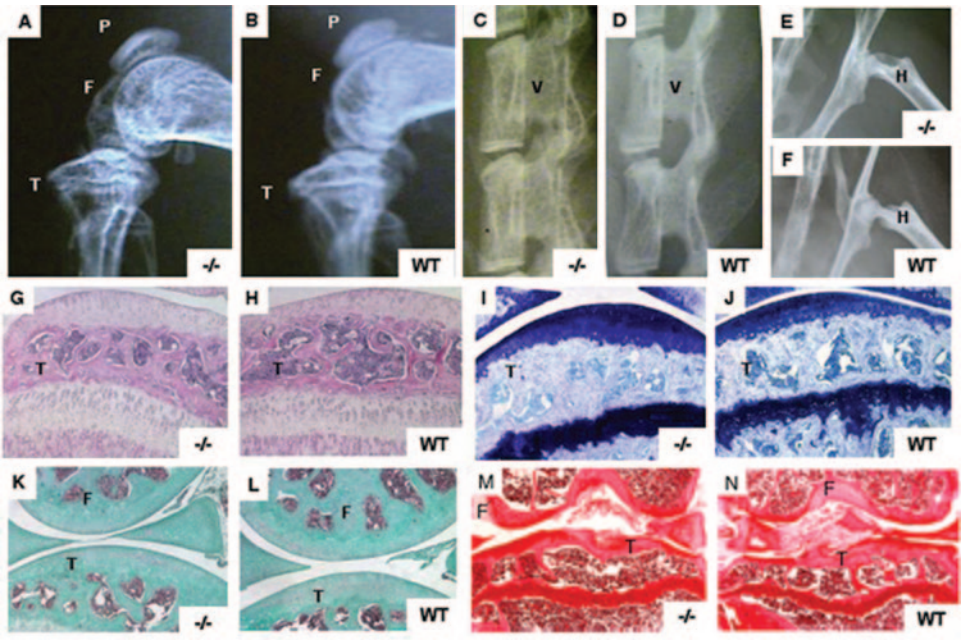

FIG. 3. Radiologic and histological analyses of wild-type (WT) and *Wisp3*$^{-/-}$ mice. (A to F) Radiographs comparing 4-month-old *Wisp3*$^{-/-}$ and WT mice knee joints (A and B), spines (C and D), and hips (E and F) are indistinguishable. (G to N) Sagittal sections of knee joints stained with hematoxylin and eosin in 1-month-old mice (G and H), toluidine blue in 9-month-old mice (I and J), Goldner's trichrome in 1-year-old mice (K and L), and coronal sections stained with safranin O in 24-month-old mice (M and N). F, femoral condyle; T, tibial plateau; V, vertebra; H, proximal femur by femoral head. Magnification, ×100 (G to N).

to their littermates, with all three genotypes able to live beyond 2 years of age. Although the targeting strategy was predicted to create an allele whose expression could be detected following staining for β-galactosidase activity, we remained unable to identify *Wisp3-lacZ* expression in developing embryos, developing limbs, or articular cartilage from the targeted mice (data not shown).

***Wisp3*$^{-/-}$ mice have no phenotypic features of PPD.** *Wisp3*$^{-/-}$ mice had no birth defects and were clinically indistinguishable from wild-type littermates. Radiologic analysis of *Wisp3*$^{-/-}$ mice at 4 months of age showed no evidence of skeletal abnormalities (Fig. 3A to F), and no signs of joint disease (swelling, restricted motion, and altered gait) were seen even at 2 years of age (data not shown). Histological analyses of knee joints from 1-, 9-, 12-, and 24-month-old *Wisp3*$^{-/-}$ animals were indistinguishable from those of wild-type mice by a variety of staining methods (Fig. 3G to N).

In humans and in mice, chondrocytes within the epiphyses of long bones undergo hypertrophy, leading to the formation of secondary centers of ossification (6). Children with PPD have more mature-appearing secondary centers of ossification than do age- and gender-matched controls (Fig. 4A and B), suggesting that Wisp3 may regulate the onset of bone formation at these sites. Therefore, we compared the appearance of secondary centers of ossification in *Wisp3*$^{+/+}$ and *Wisp3*$^{-/-}$ mice. To examine secondary centers of ossification, 7-day-old pups were sacrificed, and their skeletons were stained with Alcian blue and alizarin red. Variation in the pattern of ossification was present in the front and hind paws and knees of mice within each genotype class (Fig. 4C to J and data not shown); however, we did not find any genotype-specific differences in the ossification pattern.

Laboratory mice and humans differ with respect to activities of daily living and the stress each places on their joints. To determine whether mice lacking Wisp3 were less able to respond to added physical stress than wild-type littermates, we isolated 15 wild-type and 23 *Wisp3*$^{-/-}$ males at 2 months of age and gave them ad libitum access to running wheels for another 8 or 12 months. Voluntary running times (in hours) and distances (in kilometers) were recorded daily. No genotype-specific differences in running wheel use were observed between wild-type and *Wisp3*$^{-/-}$ mice (data not shown).

Following sacrifice, the running wheel mice were subjected to radiologic analysis, and their knee joints were subjected to histological analysis. Among mice that ran for 8 months, 0 of 7 wild-type and 3 of 10 *Wisp3*$^{-/-}$ mice developed severe osteoarthritis. While this result implies a possible difference in wild-type and mutant mice's ability to respond to cartilage stress, this cohort size is too small to be statistically significant at P values of <0.05. Among mice that ran for 12 months, 6 of 8 (75%) wild-type mice and 9 of 13 (69%) *Wisp3*$^{-/-}$ mice had histological evidence of osteoarthritis, including loss of proteoglycan, fibrillation or denuding of the joint surface, synovial hyperplasia, and chondrification of noncartilaginous tissues (Fig. 5). In the 12-month cohort, there were no radiologic or histological differences in the severity of cartilage damage between the wild-type and *Wisp3*$^{-/-}$ mice, and the pathological changes were similar to those described in other mouse models of osteoarthritis (14, 18, 28).

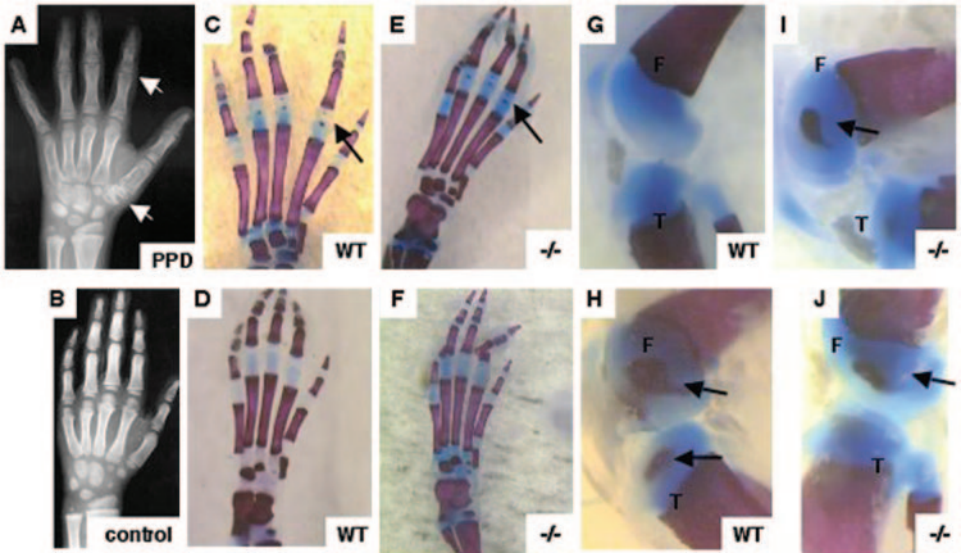

FIG. 4. Secondary centers of ossification in wild-type (WT) and *Wisp3*$^{-/-}$ mice. (A and B) Hand radiographs of an 8-year-old patient with PPD showing enlarged epiphyses within phalanges and carpal bones (white arrows) compared to an age- and gender-matched control. (C to J) Alcian blue-stained (cartilage) and alizarin red-stained (bone) 7-day-old wild-type and *Wisp3*$^{-/-}$ mouse hind paws (C to F) and knee joints (G to J) do not reveal genotype-specific effects on secondary centers of ossification. Black arrows indicate epiphyseal centers. F, femoral condyle; T, tibial plateau. Magnification, ×8 (G to J) and ×10 (C to F).

Overexpression of human WISP3 in mouse cartilage. Since *Wisp3*$^{-/-}$ mice had no detectable phenotype, we next asked whether overexpression of WISP3 would have phenotypic consequences, thereby suggesting a biological function for this protein. Several transgenic mouse lines that express human WISP3 under the control of the type II collagen promoter and enhancer were created using the cartilage-specific expression vector pKN185 (Fig. 6A), which has been previously characterized (7, 13). One line, *WISP3*^{TG}, which contains approximately 10 copies of the transgene (Fig. 6C) and carries *WISP3* mRNA in cartilage detectable by Northern blotting and protein in cartilage detectable by Western blotting, was studied further (Fig. 6B and D).

No physical abnormalities resulted from overexpression of WISP3, since transgenic mice were indistinguishable from nontransgenic littermates. Heterozygous and homozygous transgenic offspring were born in the expected Mendelian ratios and did not differ from wild-type mice in size and weight at birth or at the time of sacrifice. Histological analysis of 4-month-old (data not shown) and 11.5-month-old transgenic mouse knee joints revealed no difference from analyses of tissue from wild-type mice (Fig. 7E and F). Our studies indicate that mice are unaffected by overexpression of human WISP3 in cartilage, at least until 1 year of age.

Immunohistochemical staining of 2-day-old wild-type, *Wisp3*$^{-/-}$, and *WISP3*^{TG} transgenic mouse elbow joints detected WISP3 protein only in the transgenic mice (Fig. 7A to D). No staining was seen when preimmune serum and/or secondary antibody was used (data not shown). Despite being generated against a human WISP3 polypeptide sequence, mouse Wisp3 differs at only 1 of the polypeptide epitope's 15 residues; the W3-C antibody had similar sensitivity in detecting

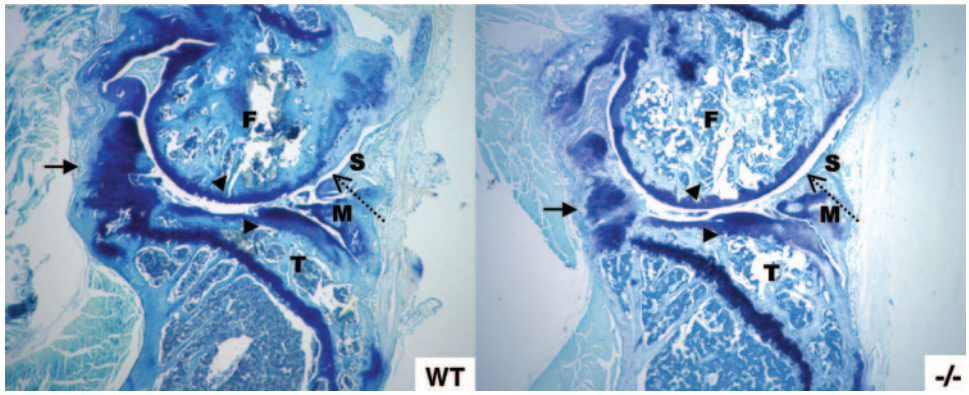

FIG. 5. The effect of exercise-induced stress on wild-type (WT) and *Wisp3*$^{-/-}$ mice. Sagittal sections stained with toluidine blue of knee joints from WT and *Wisp3*$^{-/-}$ running wheel mice reveal similar changes, including hyperplastic synovium (dashed arrow), chondrification of noncartilagenous tissues (arrow), and loss of cartilage surface (arrowheads). F, femoral condyle; T, tibial plateau; M, meniscus; S, synovium.

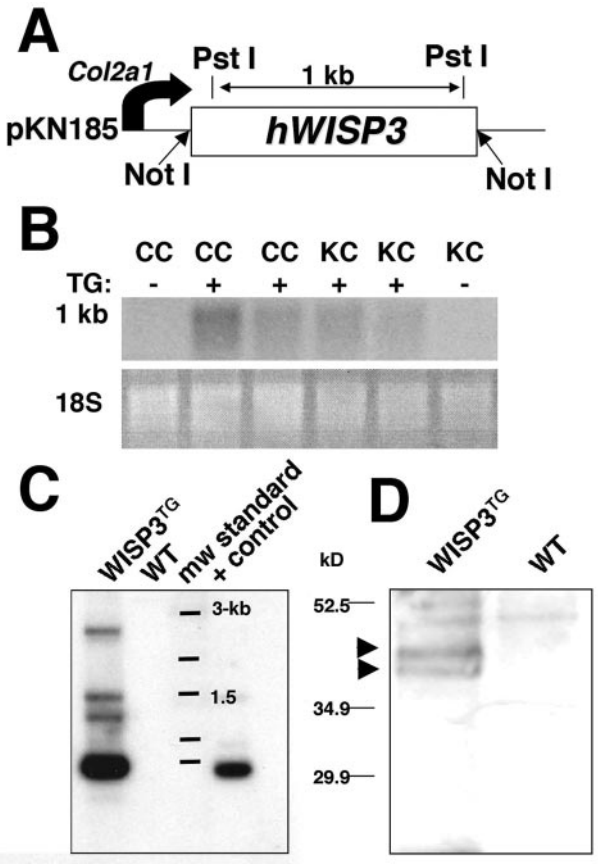

FIG. 6. Production of *WISP3*^{TG} mice and demonstration of transgene expression in cartilage. (A) Schematic depicting the transgene construct containing *WISP3* cDNA cloned with NotI restriction sites into the expression vector pKN185. PstI restriction sites and distances are noted. (B) Northern blot of costal cartilage (CC) and knee (KC) cartilage total RNA from *WISP3*^{TG} and wild-type (WT) mice demonstrate detectable expression only in transgenic mice. (C) Southern blot of PstI-digested tail DNA probed with ^{32}P-labeled full-length *WISP3* cDNA showing 1-kb transgene fragments in a *WISP3*^{TG} mouse but not in a WT mouse. WT mouse DNA spiked with transgene plasmid DNA prior to PstI digestion served as a positive control (+ control). (D) Western blot of protein extracts of femoral head cartilage from *WISP3*^{TG} and WT mice after electrophoresis in a 10% SDS–Tris HCl gel under reducing conditions. Immunodetection with the polyclonal antibody (W3-C) demonstrates full-length (~40 to 45 kDa) WISP3 protein in *WISP3*^{TG} (arrowheads) but not WT mice.

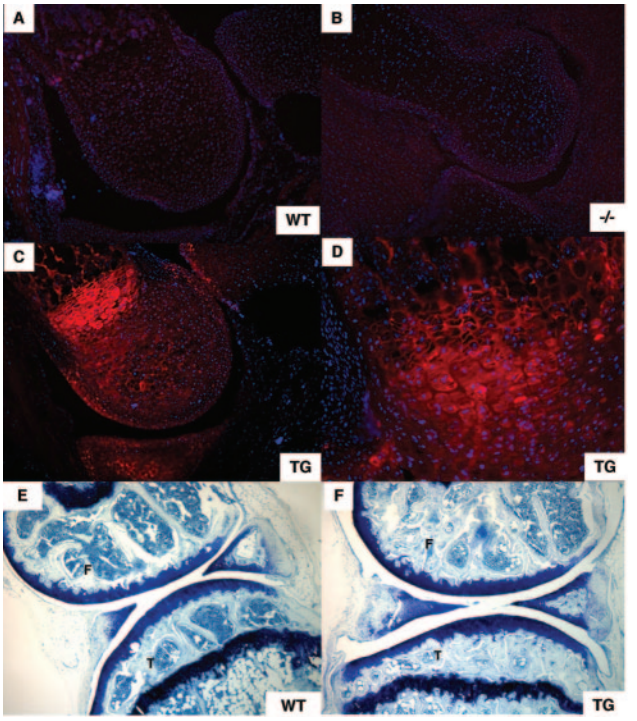

FIG. 7. Immunofluorescence and histological analyses of WT, *Wisp3*$^{-/-}$, and *WISP3*^{TG} mice. (A to D) Immunofluorescence staining of elbow joint sections from 2-day-old WT, *Wisp3*$^{-/-}$, and *WISP3*^{TG} (TG) mice with polyclonal antibody W3-C. WISP3 protein was detected with a red fluorescence-labeled secondary antibody, while cell nuclei were stained blue with DAPI. No staining was seen with WT or *Wisp3*$^{-/-}$ mice, while cartilage staining is apparent with *WISP3*^{TG} mice. Note that WISP3 protein is not detectable in noncartilagenous tissues in the joints of the *WISP3*^{TG} mice. (E and F) Comparison of toluidine blue-stained sagittal sections of 11.5-month-old WT and *WISP3*^{TG} knee joints revealed no obvious morphological or histological differences. F, femoral condyle; T, tibial plateau. Magnification, ×100 (A to C, E, and F); ×200 (D).

the human and mouse epitopes by Western blotting when the proteins were expressed recombinantly (data not shown). These data are compatible with our inability to detect *Wisp3* mRNA expression by in situ hybridization, which suggested there would be very low levels of endogenous Wisp3 protein. Interestingly, two commercially available antibodies (Santa Cruz WISP-3 (N-18) and WISP-3 (C-14) generated against human WISP3 did not detect human WISP3 protein in the transgenic mice).

DISCUSSION

WISP3 is an essential protein for the long-term integrity of human articular cartilage. Individuals who genetically lack this protein develop severe osteoarthritis in the context of a mild skeletal dysplasia (4, 8). Human clinical and radiologic data suggest that WISP3 is primarily involved in the maintenance of articular cartilage rather than in its morphogenesis, since the severity of joint pain and the rapidity of joint failure exceed that of other human skeletal dysplasias that have more severe effects upon joint formation, joint shape, or cartilage matrix assembly. To preserve joint function, cartilage must be able to resist or respond to forces placed upon it by activities of daily living. Chondrocytes are the only living cells within articular cartilage. Because they do not normally divide during adulthood, articular cartilage chondrocytes need to survive for the lifetime of the individual and they need to be able to detect changes in surface loading and matrix assembly to effectively reinforce or restructure damaged cartilage matrix (2). Anticipating that biologic pathways involved in maintaining articular cartilage function will be conserved across species, we mutated the orthologous *Wisp3* locus in mice. To our surprise, mice lacking Wisp3 develop none of the features of PPD.

We created a mutant *Wisp3* allele in mice that is comparable to the disease-causing human mutations by deleting its three most highly conserved domains. Even after allowing mice to age for more than 2 years, we have been clinically, radiologi-

cally, and histologically unable to distinguish wild-type from *Wisp3*$^{-/-}$ mice. To determine whether mutant mice were less able to respond to cartilage stress or damage than wild-type mice, we gave them ad libitum access to running wheels for 8- and 12-month periods. At the 8-month time point, the incidence of severe osteoarthritis was greater in mutants than controls, but this difference was not statistically significant. By 12 months of age, there were no clinical or histological differences in the degree of or response to knee joint damage between the wild-type and mutant mice, despite similar patterns of running wheel use. These results suggest that ad libitum running may elicit earlier-onset knee damage in *Wisp3* mutant mice, but by 12 months there are no differences between wild-type and mutant mice. This contrasts with human PPD, in which the penetrance of joint damage is 100% by young adulthood.

We excluded the existence of a second mouse *Wisp3* locus as a possible explanation for the absence of a phenotype in our mutant animals by observing only restriction fragments representing the targeted *Wisp3* allele in low-stringency Southern blots with wild-type mouse DNA and by continually examining the publicly available mouse genome sequence (http://genome.ucsc.edu). We have not yet excluded other explanations for the absence of a phenotype, such as functional compensation by another CCN family member (e.g., Ctgf), nor have we addressed the possibility that differences in articular cartilage structure between humans and mice could account for the difference in phenotypic outcome. In the adult human knee, articular cartilage is 1 to 2 mm thick on average, while mouse knee articular cartilage is only 50 μm thick (3). Since there are such large differences in cartilage thickness between humans and mice, and nutrient availability, cell density, and stress loading of articular surfaces are dependent upon cartilage thickness, mouse cartilage may inadequately model several processes that are essential to the maintenance of human cartilage. Also, patients with PPD do not have symptom onset until 3 years of age; radiologic features are often not detectable until later childhood. Consequently, were Wisp3 to function as a chondrocyte survival factor, its deficiency might not be clinically relevant in mice that have short life spans compared to humans. Conceivably, genetic modifiers on the 129/SvEv background may also obscure a *Wisp3* deficiency phenotype. However, we are also unable to distinguish 5-month-old wild-type mice from *Wisp3*$^{-/-}$ mice on the C57BL/6J background (Kutz et al., unpublished). Finally, it is tempting to speculate that *Wisp3* is becoming a pseudogene in mice because of its undetectable expression and lack of a clear phenotype. However, *WISP3* is similarly undetectable in human tissues and cell lines, yet mutation in *WISP3* is the only known cause of PPD.

Because we could not identify a biologic phenotype in *Wisp3*$^{-/-}$ mice, we sought to produce a phenotype by overexpressing human WISP3 in mouse cartilage using the type II collagen promoter and enhancer. We chose this promoter and enhancer instead of a ubiquitous promoter to avoid the risk of causing embryonic lethality in the transgenic mice and because WISP3 affects cartilage in humans. *WISP3*^{TG} mice were also indistinguishable from wild-type mice, despite producing immunodetectable WISP3 protein. It is possible that the amino acid divergence between humans and mice has caused human WISP3 to lose biologic activity in mice. Alternatively, the biologic effect of WISP3 overexpression might not be detected with standard histology or may be age-dependent.

Despite our inability to identify a phenotype in the transgenic mice, these mice have enabled us to evaluate a rabbit polyclonal antibody, W3-C, generated against a polypeptide epitope in human WISP3, which cross-reacts with recombinantly expressed epitopes from mouse and pig Wisp3 on Western blotting. We found that W3-C detects WISP3 protein in the territorial and interterritorial matrices of transgenic mice. However, the antibody does not detect endogenous Wisp3 protein in mice. The antibody also does not detect endogenous WISP3 protein in human or pig cartilage. We do not know whether our failure to detect endogenous protein is due to the protein's epitope being masked, its abundance being low, or its expression being outside of cartilage. Other investigators have used commercially available antibodies to detect human WISP3 by immunohistochemistry (23); however, these investigators did not have WISP3-deficient tissue to use as a negative control. The commercially available antibodies do not detect WISP3 protein in the transgenic mice, nor do they distinguish wild-type mice from *Wisp3*$^{-/-}$ mice. Therefore, tissue expression patterns deduced from the use of these antibodies may be incorrect.

WISP3 is a member of the CCN protein family. WISP3 is the only family member implicated in a human genetic disease, although mouse phenotypes resulting from the targeted disruption of two other family members, Ctgf and Cyr61, have been reported. *Ctgf* mutant mice die at birth from a skeletal dysplasia caused by defective growth of vasculature into the calcified zone of growth plate cartilage (9). Mice that overexpress Ctgf in cartilage develop bones that are less dense and shorter than those of their nontransgenic counterparts (16). We tested whether WISP3 could replace the function of Ctgf by breeding the *WISP3* transgene onto the *Ctgf*$^{-/-}$ background. Despite there being strong cartilage expression of WISP3 in the *Ctgf* knockout mice, there was no phenotypic rescue (data not shown).

Cyr61 knockout mice die in utero due to failed vascularization and implantation of the placenta (15). A small percentage of mutant embryos that are able to implant subsequently die from large-vessel rupture. *Cyr61*- and *Ctgf*-null mice have defective vascular invasion affecting placentation and endochondral ossification, respectively. Since vascular invasion of bone epiphyses is required for ossification, we looked for but did not find differences in secondary center formation between wild-type and *Wisp3*$^{-/-}$ mice. In humans, vascularized cartilage canals form to bring in nutrients before the initiation of epiphyseal ossification occurs, while in mice epiphyseal ossification occurs concurrent with blood vessel invasion (6). This interspecies difference in the timing of vascular invasion during secondary center formation might explain the absence of epiphyseal abnormalities in *Wisp3*$^{-/-}$ mice.

Sen and colleagues (23) have shown that the immortalized human chondrocyte lines C-28/I2 and T/C-28a2 have alterations in type II collagen and proteoglycan mRNA levels after being transiently transfected with human WISP3. We have not quantified cartilage collagen content in the wild-type and *Wisp3*$^{-/-}$ mice; however, histological studies did not reveal matrix alterations in these mice. Also, we have not observed collagen fibril abnormalities by electron microscopy in articu-

lar cartilage obtained from a patient with PPD (Kutz et al., unpublished).

Human WISP3 deficiency affects the skeleton. Other studies suggest it may also have a role in cancer progression. Loss of WISP3 expression has been observed in tissue and cell lines from women with inflammatory breast cancer (10). Somatic mutations that cause reading frameshifts at a polyadenosine tract within the WISP3 coding sequence have also been observed at higher-than-expected rates in gastrointestinal tumors from patients with mutations in the mismatch repair pathway, implying altered WISP3 expression can contribute to this neoplastic process (26). To date, we have not observed malignancies in either the *Wisp3*$^{-/-}$ or *WISP3*^{TG} mice.

It is puzzling that Wisp3 deficiency in mice does not recapitulate the human disorder PPD. Differences in life span, weight, cartilage structure, and skeletal maturation between mice and humans may explain the different phenotypic outcomes of WISP3 deficiency. Mice lacking other cartilage matrix molecules implicated in human diseases, such as cartilage oligomeric matrix protein (Comp) and matrilin3 (Matn3), also have no phenotype (11, 25). However, in contrast to PPD, which is caused by loss-of-function mutations in WISP3, the human phenotypes associated with *COMP* and *MATN3* mutants are due to dominant negative effects. Therefore, the loss-of-function mutations created in the *Comp* and *Matn3* knockout mice are not comparable to those that cause human disease. *Wisp3*$^{-/-}$ mice may provide the first example of a gene known to cause an autosomal recessive human skeletal disease phenotype that results in no phenotypic similarity when disrupted in mice.

ACKNOWLEDGMENTS

M.L.W. is an Assistant Investigator with the Howard Hughes Medical Institute. This work was supported by a Clinical Scientist Award in Translational Research from the Burroughs Wellcome Fund and NIH grant T32HD07104.

We thank Carol Fernando and Teresa Pizzuto for their technical assistance in the care and histological analysis of the mice, Pam Schwartzberg and Amy Chen for their help in generating *Wisp3* mutant mice, Brian Johnstone for his helpful scientific discussions, Heikki Helminen and Mika Hyttinen for independently analyzing the 2-year-old wild-type and *Wisp3*$^{-/-}$ mice, James Dennis for providing EM analysis of PPD patient cartilage, Yoshihiko Yamada for providing the pKN185 vector, Celina Kleer for providing the HME cell line, and Karen Lyons for providing *Ctgf* knockout mice.

REFERENCES

1. **Brigstock, D. R.** 1999. The connective tissue growth factor/cysteine-rich 61/nephroblastoma overexpressed (CCN) family. Endocr. Rev. **20:**189–206.
2. **Dewire, P., and T. Einhorn.** 2001. The joint as an organ, p. 49–68. *In* R. W. Moskowitz (ed.), Osteoarthritis: diagnosis and medical/surgical management, 3rd ed. W. B. Saunders, London, England.
3. **Eckstein, F., M. Reiser, K. H. Englmeier, and R. Putz.** 2001. In vivo morphometry and functional analysis of human articular cartilage with quantitative magnetic resonance imaging—from image to data, from data to theory. Anat. Embryol. (Berlin) **203:**147–173.
4. **Ehl, S., M. Uhl, R. Berner, L. Bonafe, A. Superti-Furga, and A. Kirchhoff.** 2004. Clinical, radiographic, and genetic diagnosis of progressive pseudorheumatoid dysplasia in a patient with severe polyarthropathy. Rheumatol. Int. **24:**53–56.
5. **el-Shanti, H. E., H. Z. Omari, and H. I. Qubain.** 1997. Progressive pseudorheumatoid dysplasia: report of a family and review. J. Med. Genet. **34:**559–563.
6. **Floyd, W. E., III, D. J. Zaleske, A. L. Schiller, C. Trahan, and H. J. Mankin.** 1987. Vascular events associated with the appearance of the secondary center of ossification in the murine distal femoral epiphysis. J. Bone Joint Surg. Am. **69:**185–190.
7. **Horton, W., T. Miyashita, K. Kohno, J. R. Hassell, and Y. Yamada.** 1987. Identification of a phenotype-specific enhancer in the first intron of the rat collagen II gene. Proc. Natl. Acad. Sci. USA **84:**8864–8868.
8. **Hurvitz, J. R., W. M. Suwairi, W. Van Hul, H. el-Shanti, A. Superti-Furga, J. Roudier, D. Holderbaum, R. M. Pauli, J. K. Herd, E. V. Van Hul, H. Rezai-Delui, E. Legius, M. Le Merrer, J. Al-Alami, S. A. Bahabri, and M. L. Warman.** 1999. Mutations in the CCN gene family member WISP3 cause progressive pseudorheumatoid dysplasia. Nat. Genet. **23:**94–98.
9. **Ivkovic, S., B. S. Yoon, S. N. Popoff, F. F. Safadi, D. E. Libuda, R. C. Stephenson, A. Daluiski, and K. M. Lyons.** 2003. Connective tissue growth factor coordinates chondrogenesis and angiogenesis during skeletal development. Development **130:**2779–2791.
10. **Kleer, C. G., Y. Zhang, Q. Pan, K. L. van Golen, Z. F. Wu, D. Livant, and S. D. Merajver.** 2002. WISP3 is a novel tumor suppressor gene of inflammatory breast cancer. Oncogene **21:**3172–3180.
11. **Ko, Y., B. Kobbe, C. Nicolae, N. Miosge, M. Paulsson, R. Wagener, and A. Aszodi.** 2004. Matrilin-3 is dispensable for mouse skeletal growth and development. Mol. Cell. Biol. **24:**1691–1699.
12. **Kozlowski, K., J. Kennedy, and I. C. Lewis.** 1986. Radiographic features of progressive pseudorheumatoid arthritis. Australas. Radiol. **30:**244–250.
13. **Krebsbach, P. H., K. Nakata, S. M. Bernier, O. Hatano, T. Miyashita, C. S. Rhodes, and Y. Yamada.** 1996. Identification of a minimum enhancer sequence for the type II collagen gene reveals several core sequence motifs in common with the link protein gene. J. Biol. Chem. **271:**4298–4303.
14. **Lapvetelainen, T., M. M. Hyttinen, A. M. Saamanen, T. Langsjo, J. Sahlman, S. Felszeghy, E. Vuorio, and H. J. Helminen.** 2002. Lifelong voluntary joint loading increases osteoarthritis in mice housing a deletion mutation in type II procollagen gene, and slightly also in non-transgenic mice. Ann. Rheum. Dis. **61:**810–817.
15. **Mo, F. E., A. G. Muntean, C. C. Chen, D. B. Stolz, S. C. Watkins, and L. F. Lau.** 2002. CYR61 (CCN1) is essential for placental development and vascular integrity. Mol. Cell. Biol. **22:**8709–8720.
16. **Nakanishi, T., T. Yamaai, M. Asano, K. Nawachi, M. Suzuki, T. Sugimoto, and M. Takigawa.** 2001. Overexpression of connective tissue growth factor/hypertrophic chondrocyte-specific gene product 24 decreases bone density in adult mice and induces dwarfism. Biochem. Biophys. Res. Commun. **281:**678–681.
17. **Oestreich, A. E.** 2002. Mega os trigonum in progressive pseudorheumatoid dysplasia. Pediatr. Radiol. **32:**46–48.
18. **Ogueta, S., I. Olazabal, I. Santos, E. Delgado-Baeza, and J. P. Garcia-Ruiz.** 2000. Transgenic mice expressing bovine GH develop arthritic disorder and self-antibodies. J. Endocrinol. **165:**321–328.
19. **Perbal, B.** 2001. The CCN family of genes: a brief history. Mol. Pathol. **54:**103–104.
20. **Perbal, B.** 2001. NOV (nephroblastoma overexpressed) and the CCN family of genes: structural and functional issues. Mol. Pathol. **54:**57–79.
21. **Rezai-Delui, H., G. Mamoori, E. Sadri-Mahvelati, and N. M. Noori.** 1994. Progressive pseudorheumatoid chondrodysplasia: a report of nine cases in three families. Skeletal Radiol. **23:**411–419.
22. **Sambrook, J., and D. W. Russell.** 2001. Molecular cloning: a laboratory manual, 3rd ed. Cold Spring Harbor Laboratory Press, Cold Spring Harbor, N.Y.
23. **Sen, M., Y. H. Cheng, M. B. Goldring, M. K. Lotz, and D. A. Carson.** 2004. WISP3-dependent regulation of type II collagen and aggrecan production in chondrocytes. Arthritis Rheum. **50:**488–497.
24. **Spranger, J., C. Albert, F. Schilling, and C. Bartsocas.** 1983. Progressive pseudorheumatoid arthropathy of childhood (PPAC): a hereditary disorder simulating juvenile rheumatoid arthritis. Am. J. Med. Genet. **14:**399–401.
25. **Svensson, L., A. Aszodi, D. Heinegard, E. B. Hunziker, F. P. Reinholt, R. Fassler, and A. Oldberg.** 2002. Cartilage oligomeric matrix protein-deficient mice have normal skeletal development. Mol. Cell. Biol. **22:**4366–4371.
26. **Thorstensen, L., R. Holm, R. A. Lothe, C. Trope, B. Carvalho, M. Sobrinho-Simoes, and R. Seruca.** 2003. WNT-inducible signaling pathway protein 3, WISP-3, is mutated in microsatellite unstable gastrointestinal carcinomas but not in endometrial carcinomas. Gastroenterology **124:**270–271.
27. **Wynne-Davies, R., C. Hall, and B. M. Ansell.** 1982. Spondylo-epiphysial dysplasia tarda with progressive arthropathy. A "new" disorder of autosomal recessive inheritance. J. Bone Joint Surg. Br. **64:**442–445.
28. **Xu, L., C. M. Flahiff, B. A. Waldman, D. Wu, B. R. Olsen, L. A. Setton, and Y. Li.** 2003. Osteoarthritis-like changes and decreased mechanical function of articular cartilage in the joints of mice with the chondrodysplasia gene (cho). Arthritis Rheum. **48:**2509–2518.